

Synthesis, Characterization and Screening of Novel Fly Ash Based Hybrid Materials Use as a Catalyst for Synthesis of Benzimidazole and Benzoxazole Derivatives

U. G. Ghoshir¹, B. H. Zaware¹, A. E. Athare¹ and A. B. Gambhire^{2*}

¹Department of Chemistry, New Arts Commerce and Science College Ahmednagar, 414001 Maharashtra, India

²Department of Chemistry, Shri Anand College, Pathardi, Dist. Ahmednagar, 414102, Maharashtra, India

*Corresponding author (e-mail: abg_chem@ymail.com)

Cost-effective mechanically and thermally activated fly ash catalysts were synthesized by doping boric acid (1, 3, 5, 7, and 9 wt. %) in the presence of 0.5 M sulphuric acid by a co-precipitation method. The synthesized hybrid materials were characterized by XRD, FT-IR, SEM-EDS and NH₃-TPD analyses. The catalytic active sites on the inert surface of fly ash were studied by synthesizing benzimidazole and benzoxazole derivatives. The optimal conditions for the highest product conversion were determined through the careful adjustment of variables such as the catalyst weight fraction, molar ratio of reactants, time and temperature. The catalyst containing 5 wt. % boric acid was found to be the most efficient and could be reused for up to four reaction cycles without loss of conversion efficiency. This study presents a potential green chemistry approach for utilizing industrial solid waste as a valuable resource.

Keywords: Fly ash-based hybrid materials; benzimidazole; benzoxazole derivatives

Received: January 2023; Accepted: March 2023

Currently, N-bearing heterocyclic structures (four-, five- and six-membered rings) such as β -lactams, pyrazoles, imidazoles, 1, 2, 4-triazoles, pyrimidines, quinolines, and quinazolines have many applications in organic synthesis. Compounds containing N and O atoms like benzimidazoles and benzoxazoles have various applications in pharmaceutical and medicinal fields due to their active role in biological systems. Heterocyclic compounds have demonstrated significant activity as agents that can counteract bacteria [1, 2] viruses [3] fungi [4], inflammation [5], and tumours [6, 7]. There are numerous methods that have been developed for synthesizing benzimidazoles and benzoxazoles. They may be prepared through a chemical reaction between o-phenylenediamines or 2-nitroanilines and carboxylic acids [8] or their derivatives (such as nitriles, imidates, or ortho-esters) [9]. In addition, benzimidazoles and benzoxazoles have been synthesized through the condensation-aromatization of o-phenylenediamines or o-aminophenol with aldehydes in the presence of various catalysts such as NaHSO₃ [10], sulfamic acid [11], FeCl₃.6H₂O [12], ZrCl₄ [13], Sc(OTf)₃ [14], Pb(OAc)₄ [15], In(OTf)₃ [16], Heuland natural zeolite [17], NaY zeolite [18], AlKT-5 [19], Co(OH)₂/CoO (II) [20], nano In₂O₃ [21], iron (III) sulfate-silica [22], MoO₃/CeO₂-ZrO₂ [23], Fe(HSO₄)₃ [24], T₃P [25], Er(OTf)₃ [26], KCN/MWCNT [27] and TiCl₃OTf/EtOH [28]. But these methods have many drawbacks, including the use of expensive and toxic reagents, long reaction times and high synthesis temperatures. Therefore, the development of a simple, mild and efficient method would be very useful. In this study, we used a dopant

and co-dopant supported on fly ash to synergistically enhance the acidic character of the catalyst. We developed a simple, efficient and low-cost method for the synthesis of benzimidazole and benzoxazole compounds.

EXPERIMENTAL

Chemicals and Materials

o-Phenylenediamine, o-aminophenol, substituted aryl aldehydes, boric acid, ethanol, and ethyl acetate were obtained from Sigma Aldrich, and fly ash was collected from the thermal power plant in Parli Vajinath, Maharashtra, India.

Preparation of Catalyst

The collected fly ash was crushed using a ball mill and calcined at 400 °C up to 1 h in a muffle furnace. About 10 g of the fly ash was treated with 1-9 wt. % of boric acid, separately. A homogeneous slurry was prepared by adding 5 ml of 0.5 M sulfuric acid and 100 ml of deionized water to the mixture, stirring constantly for 12 h. Then, the slurry was left for aging for 5 days. The mixture was evaporated at 100 °C to obtain a dry powder, which was then calcined at 400 °C for 1 h to prepare the fly ash-based hybrid material.

Characterization

The synthesized fly ash-based hybrid material was characterized using X-ray powder diffraction (XRD)

at room temperature using a Bruker AXS D8 model with monochromatic Cu radiation (40 kV, 30 mA). The particle sizes of the materials were determined by X-ray powder diffraction based on the maximum intensity peaks. Surface morphology and elemental analysis of the samples were performed using an energy dispersive spectrophotometer (EDS) (Jeol; JED-2300), while temperature programmed desorption (NH₃-TPD) was performed on a chemisorption analyzer (Autosorb-iQ-C, Quantachrome Instruments). The acidity determination was supported by TGA studies using 2, 6 dimethylpyridine at room temperature for 24 h which was then subjected to thermal analysis under a N₂ atmosphere at a heating rate of 10 °C min⁻¹. The fraction of weight loss in the range of 300-600 °C was calculated and taken as a measure of the Bronsted acidity of the samples. FT-IR analysis of samples were carried out using a Shimadzu-8400 spectrometer in the

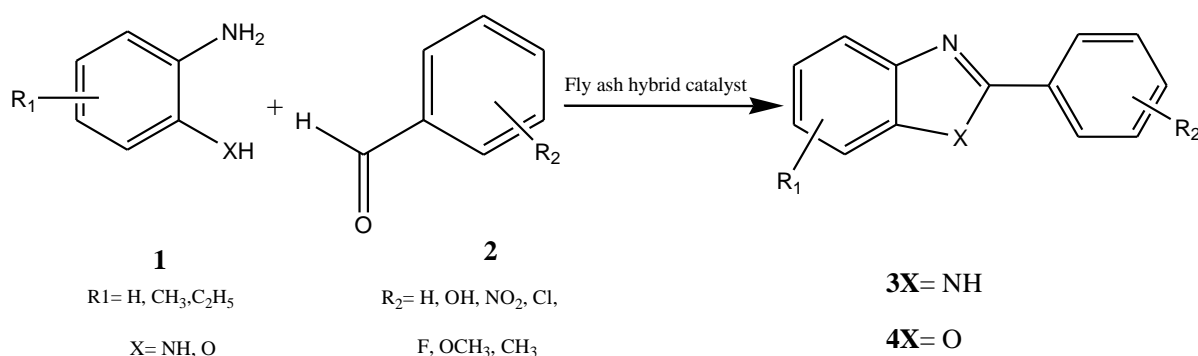
range of 4000-400 cm⁻¹.

Catalytic Activity

The catalytic activity of the synthesized fly ash-based hybrid materials was tested in the synthesis of benzimidazole or benzoxazole using *o*-phenylenediamine or *o*-aminophenol with substituted aryl aldehydes, respectively, as described in Scheme I and Tables 1 and 2.

Screening of Catalyst

Table 3 summarizes the results of the screening of fly ash-based hybrid materials for their ability to catalyse the synthesis of heterocyclic benzimidazole and benzoxazole through the use of appropriate reaction conditions.



Scheme I. Synthesis of benzimidazole and benzoxazole using various fly ash-based hybrid materials from *o*-phenylenediamine and *o*-aminophenol with aryl aldehyde.

Table 1. Synthesis of benzimidazole derivatives from substituted *o*-phenylenediamine with substituted aryl aldehyde using 5 wt. % H₃BO₃/fly ash.

Entry	R ₁	R ₂	Product (3X)	Time (min)	Yield (%)
1	H	H		5	92
2	H	OH		8	90
3	H	2-OH		10	85
4	H	4-NO ₂		5	92
5	H	3-NO ₂		7	88

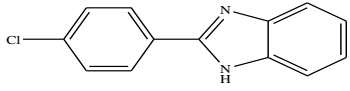
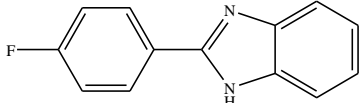
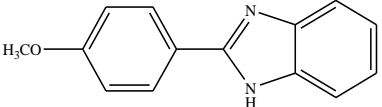
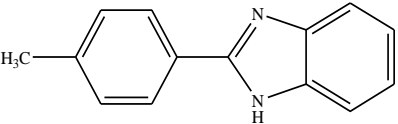
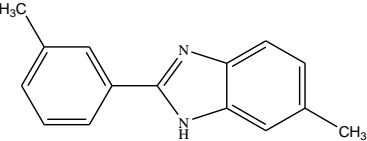
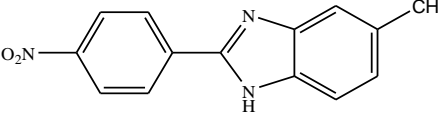
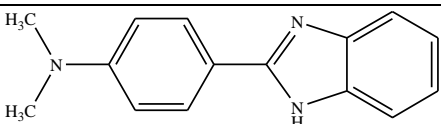
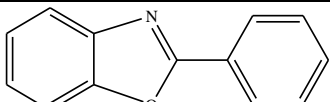
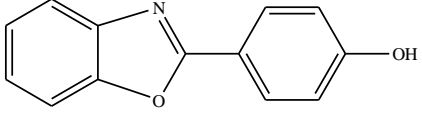
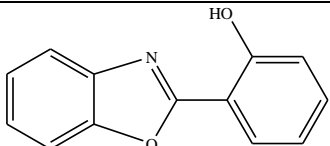
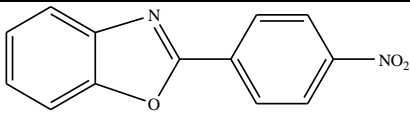
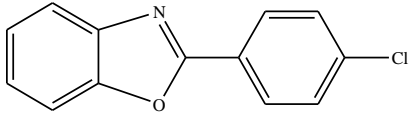
6	H	4-Cl		5	92
7	H	4-F		6	90
8	H	4-OCH ₃		5	92
9	H	4-CH ₃		5	90
10	5-CH ₃	3-CH ₃		8	88
11	5-CH ₃	4-NO ₂		6	91
12	H	4-N(CH ₃) ₂		7	87

Table 2. Synthesis of benzoxazole derivatives from substituted o-aminophenol with substituted aryl aldehyde using 5 wt. % H₃BO₃/fly ash.

Entry	R ₁	R ₂	Product (4X)	Time (min)	Yield (%)
1	H	H		5	90
2	H	4-OH		7	87
3	H	2-OH		8	84
4	H	4-NO ₂		5	90
5	H	4-Cl		5	90

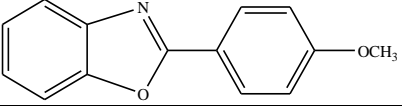
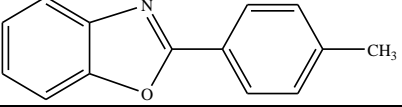
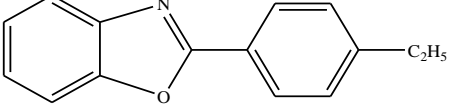
6	H	4 - OCH ₃		5	90
7	H	4 - CH ₃		5	89
8	H	4- C ₂ H ₅		7	86

Table 3. Screening of catalysts for the synthesis of benzimidazole and benzoxazole derivatives.

No.	Fly ash-based Catalysts	Amount of catalyst loaded (mg)	Reaction rate (min)	Yield (%)	
				Benzimidazole	Benzoxazole
1	H ₂ SO ₄ /fly ash	30	25	75	72
2	1 wt. % H ₃ BO ₃ /fly ash	30	15	80	78
3	3 wt. % H ₃ BO ₃ /fly ash	30	10	85	87
4	5 wt. % H ₃ BO ₃ /fly ash	30	5	92	90
5	7 wt. % H ₃ BO ₃ /fly ash	30	5	92	90
6	9 wt. % H ₃ BO ₃ /fly ash	30	5	91	89

General Method for Synthesis of Benzimidazole and Benzoxazole

A mixture of o-phenylenediamine or o-aminophenol (1 mmole), substituted aryl aldehyde (1 mmole) and co-doped fly ash-based hybrid material (30 mg) in ethanol (5 ml) was placed in a round bottom flask and stirred at room temperature. The reaction was monitored by TLC. After completion of the reaction, the mixture was filtered, washed with cold water, dried and recrystallized in ethanol. Synthesized derivatives are listed in Tables 1 and 2 with their yields, rates and physical parameters.

Spectral Analysis1) **5-Methyl-2-(3-methylphenyl)-1H-benzimidazol (Table 1, entry 10)**

¹H NMR (CDCl₃) : δ 9.7 (s, 1H, N-H), 7.9 (s, 1H, Ar-H), 7.9 (s, 1H, Ar-H), 7.5 (d, J = 8.0 Hz, 1H, Ar-H), 7.4 (s, 1H, Ar-H), 7.2 - 7.2 (m, 1H, Ar-H), 7.1 (d, J = 7.6 Hz, 1H, Ar-H), 7.0 (d, J = 8.4 Hz, 1H, Ar-H), 2.4 (s, 3H, -CH₃) and 2.2 (s, 3H, -CH₃).

¹³C NMR (CDCl₃) : δ 151.9, 138.8, 138.7, 137.6, 132.8, 130.8, 129.7, 128.9, 127.5, 124.4, 123.8, 115.1, 114.5, 21.7 and 21.2.

Mass (EI, m/z) : 223.12 [M⁺]

2) **5-methyl-2-(4-nitrophenyl)-1H-benzimidazole (Table 1, entry 11)**

IR (KBr pellet) : ν_{max} 3109, 1605, 1511, 1463, 1354, 1176, 739, 701 and 657 cm⁻¹.

¹H NMR (DMSO-d₆) : δ 8.36 (s, 4H, 1H, overlapped Ar-H and N-H), 7.4 (s, 1H, Ar-H), 7.5 (d, J = 8.0 Hz, 1H, Ar-H), 2.4 (s, 3H, -CH₃), and 7.08 (d, J = 8.3 Hz, 1H, Ar-H).

¹³C NMR (DMSO-d₆) : δ 159.0, 153.7, 143.2, 136.3, 131.0, 129.3, 127.9, 119.4, 114.7, 114.6, 111.5 and 31.

Mass (EI, m/z) : 254 [M⁺]

3) **2-(4-Methylphenyl)benzoxazole (Table 2, entry 7)**

¹H NMR (CDCl₃) : δ 8.18 (d, J = 8 Hz, 2H, Ar-H), 7.7 (m, 1H, Ar-H), 7.62 (m, 1H, Ar-H), 7.39 (d, J = 8.7 Hz, 4H, Ar-H) and δ 2.47 (s, 3H, -CH₃).

¹³C NMR (CDCl₃) : δ 163.2, 150.8, 142.2, 129.6, 127.5, 124.8, 124.5, 119.7, 110.5 and 21.4.

4) **2-(4-ethylphenyl)benzoxazole (Table 2, entry 8)**

IR (KBr pellet) : ν_{max} 3320, 3230, 2349, 1640, 1573, 1451, 1366, 1273, 1196, 1159, 1067, 832, 797 and 749 cm⁻¹

¹H NMR (DMSO-d₆) : δ 8.2 (d, J = 7.4 Hz, 2H, Ar-H), 7.6-7.5 (m, 4H, Ar-H), 7.5 (d, J = 7.4 Hz, 1H, Ar-H), 7.4 (t, J = 7.6 Hz, 1H, Ar-H), 7.06 (d, J = 8.2 Hz, 1H, Ar-H), 2.7-2.6 (m, 2H, -CH₂-CH₃) and 1.24 (t, J = 7.2 Hz, 3H, -CH₂-CH₃).

¹³C NMR (DMSO-d₆) : δ 151.5, 138.5, 138.0, 132.3, 130.9, 130.6, 130.3, 130.1, 129.4, 126.8, 123.0, 29.0 and 16.8.

Mass (EI, m/z) : 223.12 [M+]

RESULTS AND DISCUSSION

XRD Study

To understand the phase symmetry of the synthesized samples, a systematic XRD study was conducted. Figure 1(a) shows the XRD pattern of pure fly ash calcined at 400 °C for 1 h in air. Sharp peaks at 2θ

= 20.97° and 26.77° corresponding to (111) and (021) can be observed, which are associated with the monoclinic crystalline structure of fly ash [ASTM card No-86-0680] [29]. Figure 1(b) shows the XRD pattern of H₂SO₄-doped fly ash, which exhibits a crystalline phase of silico-aluminate species that was reduced to an amorphous phase possibly due to the interaction between the anions of sulfuric acid and the silanol groups present on the surface of the fly ash. Figure 2 shows the XRD pattern of (c) 1 wt. % H₃BO₃/fly ash, (d) 3 wt.% H₃BO₃/fly ash, (e) 5 wt. % H₃BO₃/fly ash (f) 7 wt.% H₃BO₃/fly ash, and (g) 9 wt. % H₃BO₃/fly ash powders with a fixed amount of H₂SO₄, calcined at 400 °C for 1 h. A single monoclinic structure with a crystalline phase was obtained for the entire range of H₃BO₃ concentrations. It was observed that the peak intensity of the doped fly ash increased due to the direct synergistic effect on the silica-alumina species in the fly ash. The average particle sizes of the samples at the major peaks were calculated using the Debye-Scherrer formula based on XRD peak broadening analysis techniques. The particle size was found to be as large as 60-85 nm for 1 wt. %, 3 wt. %, 7 wt. % and 9% wt. H₃BO₃/fly ash, and as small as 40 nm for the 5 wt. % H₃BO₃/fly ash. This apparent fall in the particle size should ensure high catalytic activity for the sample with 5 wt. % H₃BO₃, if it is used for catalytic applications. We doped 1-9 wt. % H₃BO₃ to enhance the surface area of catalyst. However, we observed a drastic fall in the particle size with 5 wt. % H₃BO₃, because for this wt. % of H₃BO₃ in activated fly ash, the grain boundary inhibits crystallite growth of the catalyst, thus reducing its particle size.

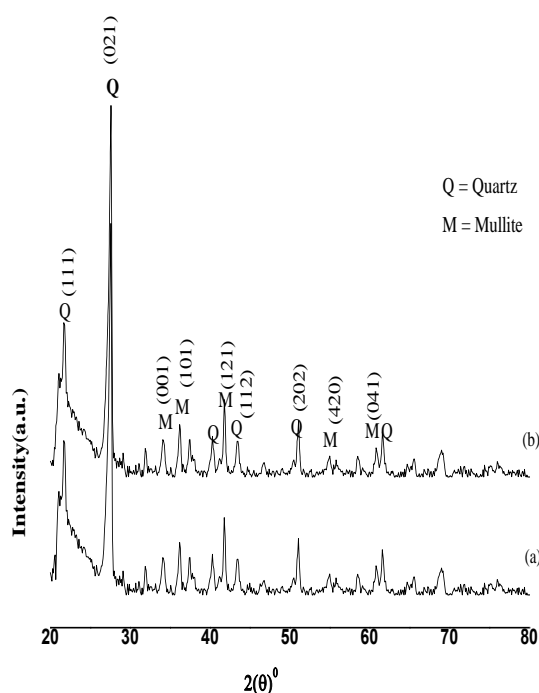


Figure 1. X-ray diffraction patterns of (a) pure fly ash, and (b) H₂SO₄/fly ash calcined at 400 °C for 1 h.

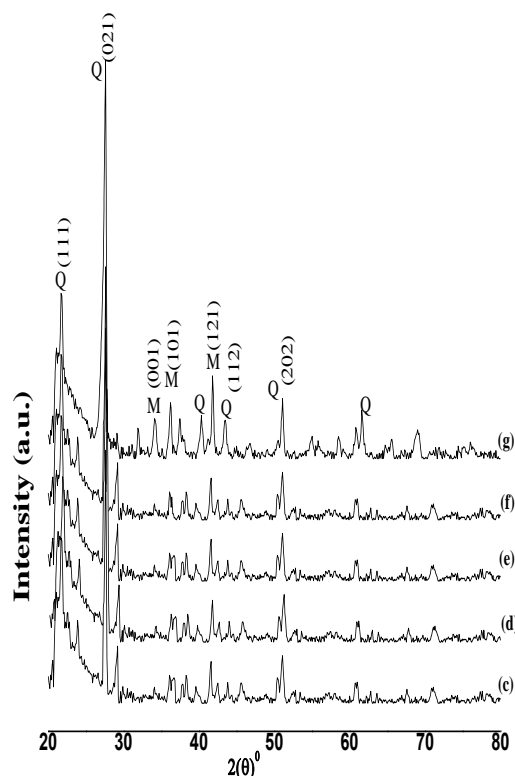


Figure 2. X-ray diffraction patterns of (c) 1 wt. % H_3BO_3 /fly ash, (d) 3 wt.% H_3BO_3 /fly ash, (e) 5 wt.% H_3BO_3 /fly ash, (f) 7 wt.% H_3BO_3 /fly ash, and (g) 9 wt. % H_3BO_3 /fly ash powders with a fixed amount of H_3BO_3 , calcined at $400\text{ }^\circ\text{C}$ for 1 h.

FT-IR

Figure 3 shows the FT-IR spectra of (a) pure fly ash, and (b) H_2SO_4 /fly ash while Figure 4 shows the FT-IR spectra of (c) 1 wt. % H_3BO_3 /fly ash, (d) 3 wt.% H_3BO_3 /fly ash, (e) 5 wt.% H_3BO_3 /fly ash, (f) 7 wt.% H_3BO_3 /fly ash, and (g) 9 wt. % H_3BO_3 /fly ash samples, all in the range of 4000 to 500 cm^{-1} . The band corresponding to surface hydroxyl groups appears at $3300\text{--}3000\text{ cm}^{-1}$. This indicates the presence of strong hydrogen bonding in the samples, as indicated by the broad band [31], which is attributed to the surface Si-OH groups and absorbed water molecules on the surface [30]. The intense peak observed in the region of $1000\text{--}1300\text{ cm}^{-1}$ is attributed to the valence vibration of the silicate oxygen skeleton (Si-O-Si). After acid treatment, the increase in silica content resulted in a distinct and significant increase in the broadening of the -OH peak at 3000 cm^{-1} in all

samples in comparison to pure fly ash, as shown in Figure 4. This suggests that the increase in surface hydroxyl groups [32] is due to the acid treatment, which enhanced the silica content. After acid treatment, an intense band was observed in the range of $1050\text{--}1350\text{ cm}^{-1}$, which is usually assigned to the valence vibration of the silicate oxygen skeleton and corresponds to the amorphous silica content. This indicates an increase in amorphous silica content after acid treatment. The region between $800\text{--}500\text{ cm}^{-1}$ shows the symmetric stretching of Si-O-Si and Al-O-Si bonds, which corresponds to the formation of amorphous to semi-crystalline alumina-silicate materials. The band below 500 cm^{-1} shows the bending vibration of Si-O-Si and O-Si-O bands [33]. The increase in silica content and surface hydroxyl groups is responsible for the development of acidic sites on the catalyst, which helps to enhance catalytic activity.

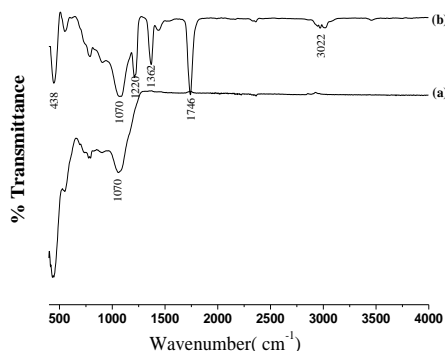


Figure 3. FT-IR spectra of (a) pure fly ash, (b) H_2SO_4 /fly ash calcined at $400\text{ }^\circ\text{C}$ for 1 h.

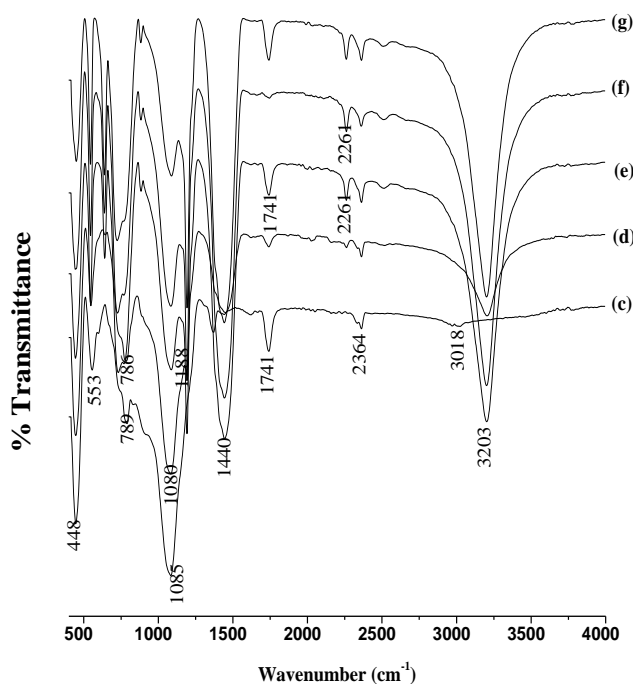
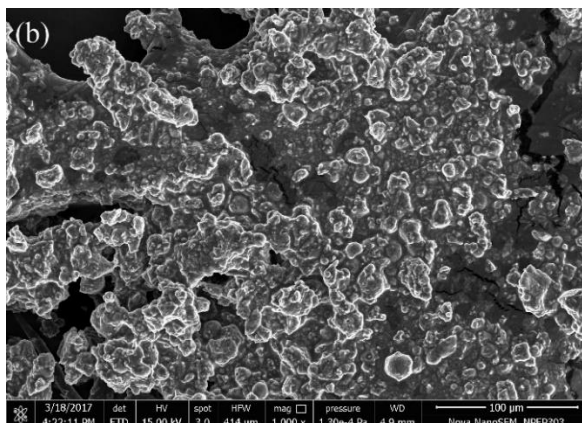
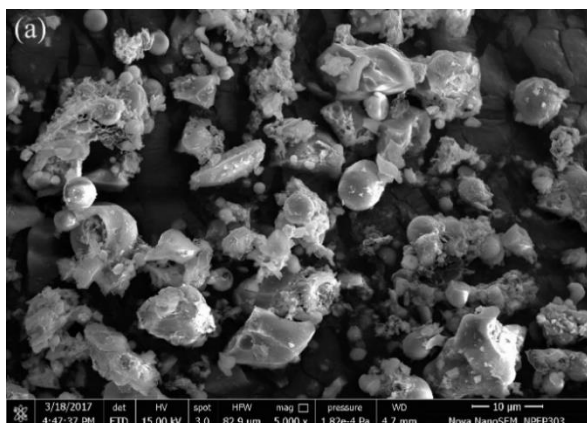


Figure 4. FT-IR spectra of (c) 1 wt. % H_3BO_3 /fly ash, (d) 3 wt. % H_3BO_3 /fly ash, (e) 5 wt. % H_3BO_3 /fly ash, (f) 7 wt. % H_3BO_3 /fly ash, and (g) 9 wt. % H_3BO_3 /fly ash powder with a fixed amount of H_2SO_4 calcined at $400\text{ }^\circ\text{C}$ for 1 h.

SEM-EDS Analysis

The effect of the dopant and co-dopant on the morphology of the synthesized samples was investigated using a scanning electron microscope (SEM). Figure 5 shows SEM images of (a) 1 wt. % H_3BO_3 /fly ash, (b) 3 wt. % H_3BO_3 /fly ash, (c) 5 wt. % H_3BO_3 /fly ash (d) 7 wt. % H_3BO_3 /fly ash and (e) 9 wt. % H_3BO_3 /fly ash calcined at $400\text{ }^\circ\text{C}$ for 1 h. The surface morphology of the fly ash samples doped with 1, 3, 7, and 9 wt. % of H_3BO_3 were found to have irregular shapes and were clumped together, with an average primary

particle size of less than 100 nm. However, the fly ash sample doped with 5 wt. % of H_3BO_3 had regular shaped particles with sizes less than 40 nm. These results are inconsistent with the XRD analysis. Chemical analysis of the elements confirmed the presence of Si, Al, O, C, Ca, Fe, K, Mg and Ti in the sample, as listed in Table 4. From these values it is clear that the percentage of Al, Si and O in the 5 wt. % H_3BO_3 /fly ash sample was found to be higher in comparison with pure fly ash. The increase in the silica-alumina content corresponds to the increase in surface hydroxyl groups on the catalyst surface. These results are consistent with the FT-IR data.



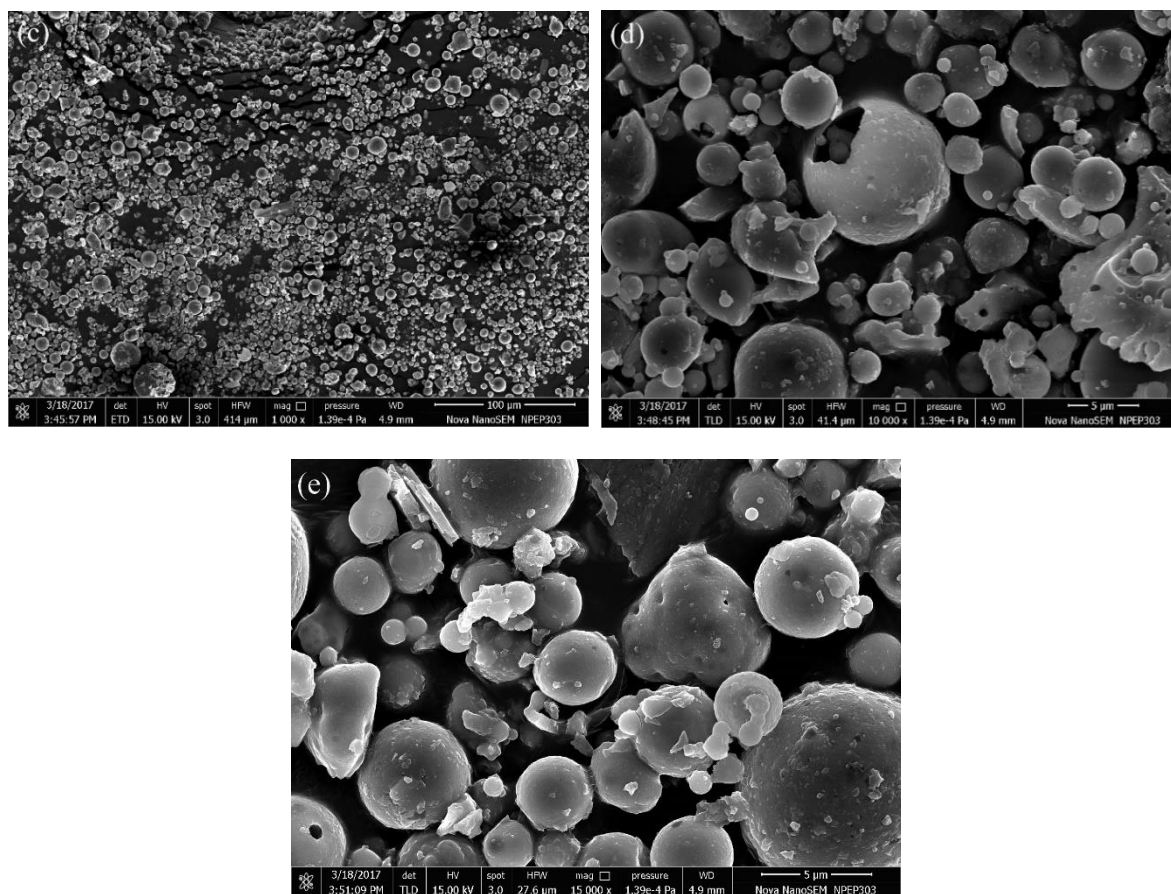


Figure 5. SEM micrographs of (a) 1 wt. % H_3BO_3 /fly ash, (b) 3 wt. % H_3BO_3 /fly ash, (c) 5 wt. % H_3BO_3 /fly ash, (d) 7 wt. % H_3BO_3 /fly ash and (e) 9 wt. % H_3BO_3 /fly ash calcined at 400 °C for 1 h.

Table 4. EDS analysis of pure and 5 wt. % H_3BO_3 /fly ash calcined at 400 °C for 1 h.

Elements	Si	Al	O	C	Ca	Fe	K	Mg	Ti	Cu	Zn	Zr	Total
Pure Fly ash Wt. (%)	3.63	2.31	47.96	45.28	0.16	0.68	0.09	0.11	0.08	0.09	0.08	0.03	100
5 wt. % H_3BO_3 /fly ash At. (%)	24.53	11.19	54.90	3.08	0.75	2.28	2.06	0.55	0.66	-	-	-	100

NH₃ - Adsorption Measurement

The acidity of the catalyst was determined with the help of a very special technique, temperature-programmed desorption of ammonia (TPD). The amount of ammonia that was removed from the catalyst during this process was measured and the results are reported in Table 5.

Table 5 shows that the total acidity of the H_2SO_4 /fly ash was 0.379 mmol/g. The values for fly ash doped with 1, 3, 7, and 9 wt. % of H_3BO_3 were 0.395 mmol/g, 0.416 mmol/g, 0.420 mmol/g and 0.426 mmol/g respectively, while for 5 wt. % H_3BO_3 /fly ash it was 0.431 mmol/g due to the synergistic effect of boric and sulphuric acids with the fly ash surface. From the above values, it can be

concluded that the catalysts on the surface of the fly ash showed sufficient acidic character to carry out the synthesis of benzimidazole and benzoxazole derivatives from o-phenylenediamine and o-aminophenol.

Catalytic Performance

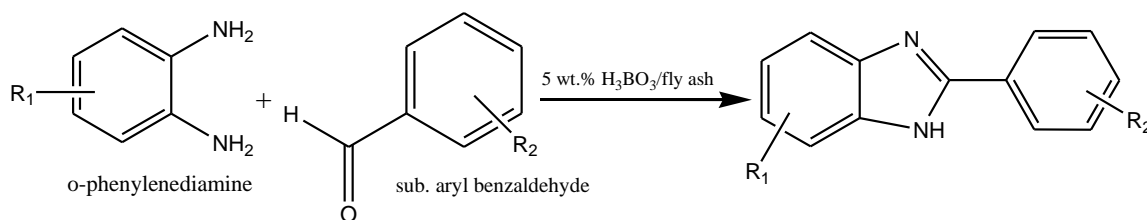
The active fly ash was used as a catalyst in the synthesis of benzimidazole and benzoxazole derivatives from o-phenylenediamine and o-aminophenol, respectively, in the presence of an aryl aldehyde. We found that the 5 wt. % H_3BO_3 /fly ash catalyst had a faster reaction rate compared to the other prepared catalysts, as shown in Table 3. This is likely due to the strong acidity of the catalyst, which is the result of a synergistic interaction between boric and sulfuric acids, making it more

effective than the other hybrid catalysts, as has been proved by the reaction rate and yield obtained. This prepared material has the potential to be used widely in organic synthesis reactions due to its activity, ease of preparation and availability of raw materials. In the synthesis of benzimidazole and benzoxazole derivatives (as shown in Scheme II and III), fly ash-based hybrid materials were

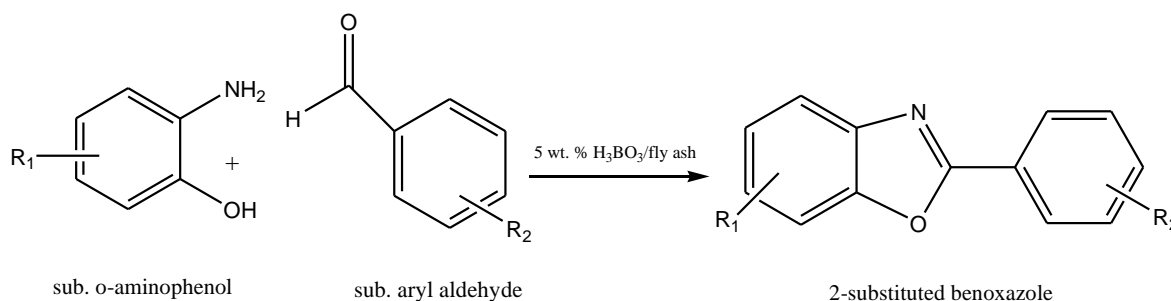
used under optimized reaction conditions and bearing electron-donating groups such as methoxy-, hydroxyl-, methyl- and N, N dimethyl-, as well as electron-withdrawing groups such as nitro-, chloro- and fluoro- substituents on the aldehyde. The yields of the heterocyclic derivatives and the reaction rates are presented in Tables 1 and 2.

Table 5. Acidity of synthesized catalysts measured by NH_3 -TPD.

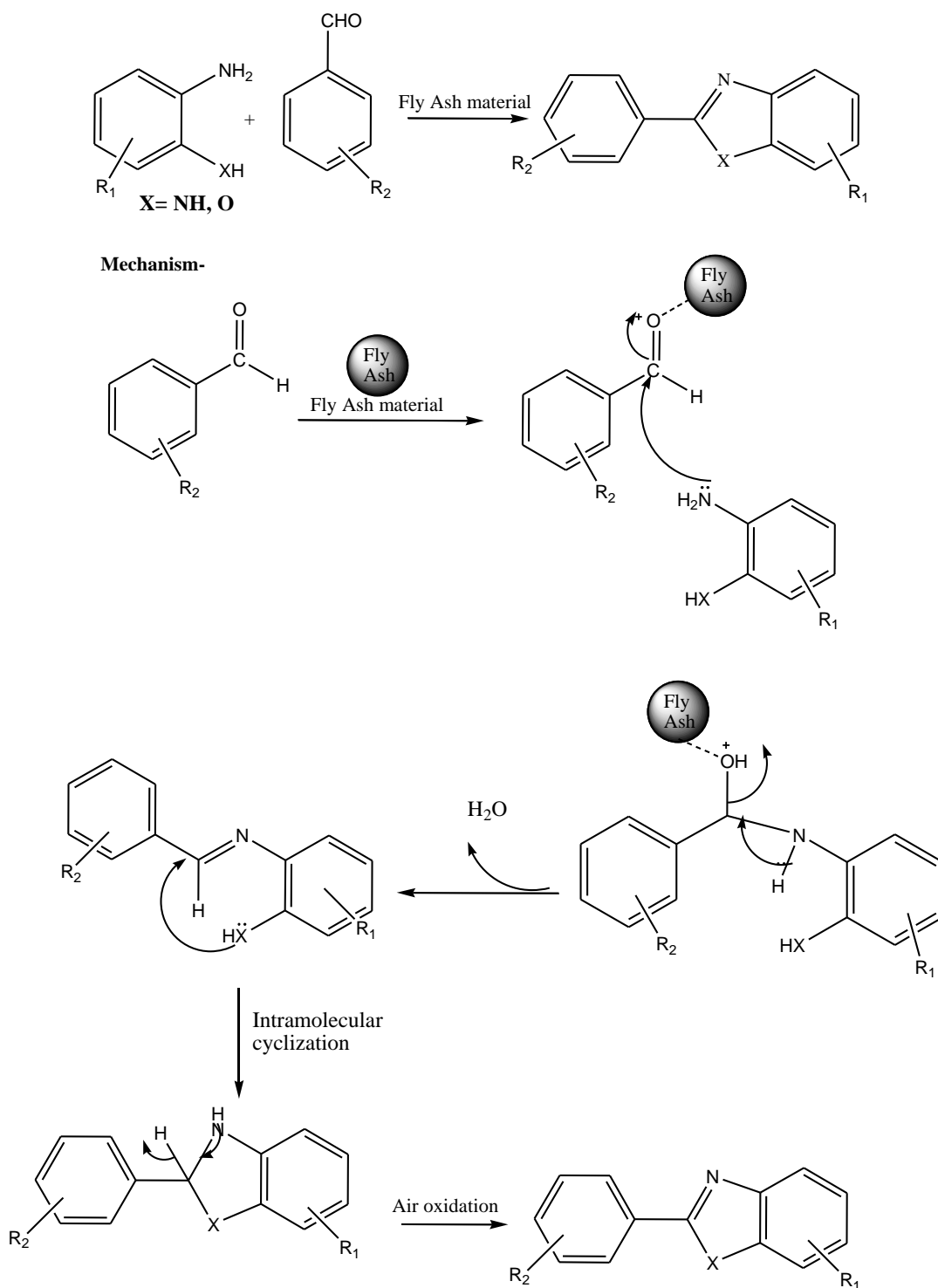
Fly ash-based Catalyst	Acidic sites (mmol NH_3/g)		
	T1 (< 200 °C)	T2 (>500 °C)	Total
$\text{H}_2\text{SO}_4/\text{fly ash}$	0.196	0.183	0.379
1 wt. % $\text{H}_3\text{BO}_3/\text{fly ash}$	0.206	0.189	0.395
3 wt. % $\text{H}_3\text{BO}_3/\text{fly ash}$	0.214	0.202	0.416
5 wt. % $\text{H}_3\text{BO}_3/\text{fly ash}$	0.227	0.204	0.431
7 wt. % $\text{H}_3\text{BO}_3/\text{fly ash}$	0.223	0.197	0.420
9 wt. % $\text{H}_3\text{BO}_3/\text{fly ash}$	0.224	0.202	0.426



Scheme II. Synthesis of benzimidazole from o-phenylenediamine with aryl aldehyde using 5 wt. % $\text{H}_3\text{BO}_3/\text{fly ash}$.



Scheme III. Synthesis of benzoxazole from o-aminophenol with aryl aldehyde using 5 wt. % $\text{H}_3\text{BO}_3/\text{fly ash}$.



Scheme IV. Possible mechanism for the synthesis of benzimidazole and benzoxazole derivatives using 5 wt. % H_3BO_3 /fly ash.

Table 6. Reusability of the catalyst the reaction of benzimidazole and benzoxazole in the presence of 5 wt. % H_3BO_3 /fly ash.

Run	1	2	3	4
Yield (%)	92	92	91	90

The reusability and recovery of the fly ash-based hybrid catalyst was investigated, as this is an important aspect for commercial applications. During the synthesis of benzimidazole and benzoxazole, the recyclability of the catalyst was tested by separating it and washing it with ethyl acetate before drying it in an oven at 110 °C for 1 h. The catalyst was then reused for further reactions, which showed equal catalytic activity up to the fourth reaction cycle and resulted in improved yields, as shown in Table 6.

Proposed Mechanism

The mechanism for 2-aryl substituted benzimidazole/benzoxazole formation is proposed in Scheme IV. Fly ash-based hybrid materials appear to play a more efficient catalytic role due to their strong oxophilicity. Initially aldehyde molecules co-ordinate through their carbonyl oxygen atom to the fly ash-based material and facilitate the nucleophilic attack. The reaction between an aldehyde and amine group leads to the formation of an imine intermediate. Then, intramolecular attack by the second group on the C=N bond followed by air oxidation gives the final product.

CONCLUSION

We prepared H₃BO₃-doped fly ash materials by a co-precipitation method. The effect of H₃BO₃ wt. % was evaluated. It was found that the 5 wt. % H₃BO₃/fly ash catalyst exhibited higher catalytic activity due to a decrease in particle size (higher surface area) and its strong acidity due to the synergistic interaction of boric and sulfuric acids. This study demonstrated the use of environmental pollutants or waste materials as catalysts in the synthesis of benzimidazole and benzoxazole. These materials can be easily obtained, have high yields, and are reusable heterogeneous catalysts.

ACKNOWLEDGEMENTS

The authors are grateful to the Research Centre, New Arts Commerce and Science College Ahmednagar for providing the laboratory facilities and would also like to thank Savitribai Phule Pune University for the characterization of the synthesized materials and analysis of the products.

ORCID

Udhav G Ghoshir <https://orcid.org/0000-0002-7003-0008>.

Compliance with Ethical Standards, Conflict of Interest

The authors declare no conflict of interest, financial or otherwise.

Ethics approval and consent to participate.

This research did not require ethical approval as it did not involve any human or animal experimentation.

Human and Animal Rights

No Animals/Humans were used for studies that are based on this research.

Consent for Publication

Not applicable.

Funding

This research received no grant from any funding agency.

REFERENCES

1. El-salam, N. M. A., Mostafa, M. S., Ahmed, G. A., Alothman, O. Y. (2013) Synthesis and Antimicrobial Activities of Some New Heterocyclic Compounds Based on 6-Chloropyridazine-3 (2H) -thione. *J. Chem.*, 1–8.
2. Azab, M. E., Youssef, M. M., El-Bordany, E. A. (2013) Synthesis and antibacterial evaluation of novel heterocyclic compounds containing a sulfonamido moiety. *Molecules*, **18**, 832–844.
3. Salem, M. S., Sakr, S. I., El-Senousy, W. M., Madkour, H. M. F. (2013) Synthesis, antibacterial, and antiviral evaluation of new heterocycles containing the pyridine moiety. *Arch. Pharm. (Weinheim)*, **346**, 766–773.
4. Cao, X., Sun, Z., Cao, Y., Wang, R., Cai, T., Chu, W., Hu, W., Yang, Y. (2014) Design Synthesis, and Structure Activity Relationship Studies of Novel Fused Heterocycles-Linked Triazoles with Good Activity and Water Solubility. *J. Med. Chem.*, **57**, 3687–3706.
5. El-Sawy, E. R., Ebaid, M. S., Abo-Salem, H. M., Al-Sehemi, A. G., Mandour, A. H. (2013) Synthesis, anti-inflammatory, analgesic and anticonvulsant activities of some new 4,6-dimethoxy-5-(heterocycles)benzofuran starting from naturally occurring visnagin. *Arab. J. Chem.*, **7**, 914–923.
6. Chen, Y., Yu, K., Tan, N. Y., Qiu, R. H., Liu, W., Luo, N. L., Tong, L., Au, C. T., Luo, Z. Q., Yin, S. F. (2014) Synthesis, characterization and antiproliferative activity of heterocyclic hypervalent-organostimony compounds. *Eur. J. Med. Chem.*, **79**, 391–398.
7. El-Sawy, E. R., Mandour, A. H., El-Hallouty, S. M., Shaker, K. H., Abo-Salem, H. M. (2013) Synthesis, antimicrobial and anticancer activities of some new N-methylsulphonyl and N-benzene-

- sulphonyl-3-indolyl heterocycles. *1st Cancer Update, Arab. J. Chem.*, **6**, 67–78.
- Grimmet, M. R., Katritzky, A. R. and Rees, C. W. (1984) Reactivity of five-membered rings with two or more heteroatoms. *Comprehensive Heterocyclic Chemistry Pergamon Press, Oxford, UK*, **5** (4), 02.
 - Czarny, A., Wilson, W. D. and Boykin, D. W. (1996) Synthesis of mono-cationic and dicationic analogs of Hoechst 33258. *Journal of Heterocyclic Chemistry*, **33** (4), 1393–1397.
 - Ridley, H. F., Spickett, R. G. W., Timmis, G. M. (1965) A new synthesis of benzimidazoles and aza-analogs. *J. Heterocycl. Chem.*, **2**, 453–456.
 - Manas Chakrabarty, Sulakshana Karmakar, Ajanta Mukherji, Shiho Arima (2006) Application of Sulfamic Acid as an Eco-Friendly Catalyst in an Expedient Synthesis of Benzimidazoles. *Chem-Inform*, **37** (40).
 - Das, A. B., Holla, H., Srinivas, Y. (2007) Efficient (bromodimethyl)sulfonium bromide mediated synthesis of benzimidazoles. *Tetrahedron Lett.*, **48** (1), 61–64.
 - Madhukar Jeripothula (2020) Zirconium Chloride (ZrCl₄): An efficient Catalyst for the Synthesis of Benzimidazole Derivatives. *IOSR Journal of Applied Chemistry*, **6** (13), 73–76.
 - Liyan Fan, Lulu Kong and Wen Chen (2015) Highly Chemoselective Synthesis of Benzimidazoles in Sc(OTf)₃-Catalyzed System. *Journal of Heterocycles*, **91** (12), 2306.
 - Stephens, F. F., Bower, J. D. (1949) The preparation of benzimidazoles and benzoxazoles from Schiff's bases. Part I. *J. Chem. Soc.*, 2971–2972.
 - Trivedi, R., De, S. K. and Gibbs, R. A. (2006) A convenient one-pot synthesis of 2-substituted benzimidazoles, *Journal of Molecular Catalysis A*, **245** (1-2), 8–11.
 - Srinivasulu, R., Kumar, K. R., Satyanarayana, P. V. V. (2014) Facile and Efficient Method for Synthesis of Benzimidazole Derivatives Catalyzed by Zinc Triflate. *Green Sustainable Chem.*, **4**, 33–37.
 - Akbar Mobinikhaledi, Naser Forughifar, Mojgan Zendehtdel, Mahsa Jabbarpour (2008) Conversion of Aldehydes to Benzimidazoles using NaY Zeolite, Synthesis and Reactivity in Inorganic, Metal-Organic, and Nano-Metal Chemistry, **38** (4), 390–393.
 - Chari, M. A., Shobha, D., Kenawy, E. R., Deyab, S. S. A., Reddy, B. V. S., Ajayan Vinu (2010) Nano porous aluminosilicate catalyst with 3D cage-type porous structure as an efficient catalyst for the synthesis of benzimidazole derivatives. *Tetrahedron Lett.*, **51** (39), 5195–5199.
 - Chari, M. A., Shobha, D. and Sasaki, T. (2011) Room Temperature Synthesis of Benzimidazole Derivatives Using Reusable Cobalt Hydroxide and Cobalt Oxide as an Efficient Solid Catalysts. *Tetrahedron Letters*, **52**, 5575–5580.
 - Sougata Santra, Adinath Majee, Alakananda Hajra (2012) Nano indium oxide: an efficient catalyst for of 1,2-disubstituted benzimidazoles in aqueous media. *Tetrahedron Letters*, **53** (15),
 - Susmita Paul, Basudeb Basu (2012) Highly selective synthesis of libraries of 1,2-disubstituted benzimidazoles using silica gel soaked with ferric sulfate. *Tetrahedron Letters*, **53** (32), 4130–4133.
 - Dagade, S. P., Deshmukh, J. M. (2019) Recyclable Nanocrystalline Copper Based on MoO₃/SiO₂ as an Efficient Catalyst for Acylation of Amines. *Bulletin of Chemical Reaction Engineering & Catalysis*, **14** (1), 93–104.
 - Eshghi, Hossein Rahimizadeh, Mohammad Shiri, Ali Sedaghat, Parisa, (2012) One-pot Synthesis of Benzimidazoles and Benzothiazoles in the Presence of Fe(HSO₄)₃ as a New and Efficient Oxidant, *Bull. Korean Chem. Soc.*, **33** (2), 515–518.
 - Xiaoan Wen, Jamal El Bakali, Rebecca Deprez-Poulain, Benoit Deprez (2012) Efficient Propylphosphonic Anhydride T3P mediated synthesis of benzothiazoles, benzoxazoles and benzimidazoles. *Tetrahedron Letters*, **53**, 2440–2443.
 - Natividad Herrera Cano, Jorge G. Uranga, Mónica Nardi, Antonio Procopio, Daniel A. Wunderlin and Ana N. Santiago (2016) Selective and eco-friendly procedures for the synthesis of benzimidazole derivatives. The role of the Er(OTf)₃ catalyst in the reaction selectivity. *Beilstein Journal of Organic Chemistry*, **12**, 2410–2419.
 - Hossein Naeimi, Soraya Rahmatinejad, Zahra Sadat Nazif (2015) A mild convenient ultrasound assisted synthesis of 2-aryl benzoxazoles catalyzed by KCN/MWCNT as an efficient heterogeneous nanocatalyst. *Journal of the Taiwan Institute of Chemical Engineers*, 1–7.
 - Javad Azizian, Parviz Torabi, Jalil Noei (2016) Synthesis of benzimidazoles and benzoxazoles using TiCl₃OTf in ethanol at room temperature. *Tetrahedron Letters*, **57** (2), 185–188.

29. Ghoshir, U. G., Kande, S. R., Muley, G. G. and Gambhire, A. B. (2019) Synthesis and Characterization of Co-Doped Fly Ash Catalyst for Chalcone Synthesis. *Asian J. Chem.*, **31** (10), 2165–2172.
30. Deepti Jain, Chitralekha Khatri, Ashu Rani (2011) Synthesis and characterization of novel solid base catalyst from fly ash. *Fuel*, **90** (6), 2083-2088.
31. Deepti Jain, Manish Mishra, Ashu Rani (2012) Synthesis and characterization of novel amino-propylated fly ash catalyst and its beneficial application in base catalyzed Knoevenagel condensation reaction. *Fuel Processing Technology*, **95**, 119–126.
32. Anita Sharma, Khushboo Srivastava1, Vijay Devra and Ashu Rani (2012) Modification in Properties of Fly Ash through Mechanical and Chemical Activation. *American Chemical Science Journal*, **2** (4), 177–187.
33. Amir Fauzia, Muhd Fadhil Nuruddin, Ahmad B. Malkawi, Mohd Mustafa Al Bakri Abdullah (2016) Study of Fly Ash Characterization as a Cementitious Material. *Procedia Engineering*, **148**, 487–493.